

Third International Conference on Inverse Design Concepts and Optimization in Engineering Sciences (ICIDES-III), Editor: G.S. Dulikravich, Washington D.C., October 23-25, 1991.

AN INVERSE INVISCID METHOD FOR THE DESIGN OF QUASI-THREE DIMENSIONAL ROTATING TURBOMACHINERY CASCADES

BONATAKI, E. , Research Assistant
 CHAVIAROPOULOS, P., Ph.D. Research Engineer
 PAPAILIOU, K.D. , Professor

NATIONAL TECHNICAL UNIVERSITY OF ATHENS
 Lab. of Thermal Turbomachines
 P.O. Box 64069, 15710 Athens, Greece.

P.12

NA 894

ABSTRACT

A new inverse inviscid method suitable for the design of rotating blade sections lying on an arbitrary axisymmetric stream-surface with varying streamtube width is presented.

Given are the geometry of the axisymmetric stream-surface and the streamtube width variation with meridional distance, the number of blades, the inlet flow conditions, the rotational speed and the suction and pressure side velocity distributions as functions of the normalized arc-length. The flow is considered irrotational in the absolute frame of reference and compressible. The output of the computation is the blade section that satisfies the above data.

The method solves the flow equations on a (Φ, Ψ) potential function-streamfunction plane for the velocity modulus, W and the flow angle β ; the blade section shape can then be obtained as part of the physical plane geometry by integrating the flow angle distribution along streamlines. The (Φ, Ψ) plane is defined so that the monotonic behaviour of the potential function is guaranteed, even in cases with high peripheral velocities.

The method is validated on a rotating turbine case and used to design new blades. To obtain a closed blade a set of closure conditions has been developed and referred in the paper.

LIST OF SYMBOLS

$A_1 \dots A_9$	differential equation coefficients	B	constant number
m	meridional distance	β	flow angle
\bar{n}	outward unit vector	(Δn)	streamtube thickness
R	radius	θ	peripheral distance
\bar{U}	peripheral velocity	Φ	potential-type function
\bar{W}	relative velocity	Ψ	stream function

INTRODUCTION

The design method which is presented in this paper is developed in order to use the results of the meridional plane calculation and in particular the geometry of the axisymmetric flow streamtubes. The design method is, then, applied in order to specify the blade section shape lying on each axisymmetric stream-surface. The complete blade is constructed by sticking these blade section shapes in the span-wise sense, as desired.

Blade design methods have already been developed in the past, for both incompressible and compressible flows (refs [1]-[11]). However, most of them refer to plane cascade configurations only. During recent years the topic of developing blade design methodologies has received particular attention and important contributions have been published in this framework (refs [1]-[5]).

The aim of the present effort was to develop an inverse inviscid method supporting the blade optimization procedure described in reference [19] and capable to deal with the general case of an arbitrary rotating cascade. The method follows the work of Schmidt^[9] and Zannetti^[11] concerning the equations employed. However, it formulates the problem in a different way and employs different numerical techniques as well as closure conditions, for reasons explained below. A first

version of the present method, using the classical potential function/stream-function definitions was presented in reference [12]. Nevertheless, problems occurred, when the method was applied to high speed rotating cascades because of the non-monotonic behaviour of the potential function. Recently, a new version has been developed, capable of overcoming this problem. This improved version which makes use of a more appropriate definition of the potential function/stream-function plane (here referred as (Φ, Ψ)) is presented in the present paper.

POSITION OF THE PROBLEM AND DEVELOPMENT OF THE EQUATIONS

A schematic representation of a peripheral cascade is given in figure 1. The aim is to compute a closed blade section, given the stream-surface geometry, the streamtube width variation with the meridional distance (m), the approximate number of blades (N), the inlet stagnation conditions (P_{T1}, T_{T1}) and velocity vector (\vec{W}_1), the meridional position of the inlet stagnation point (m_1), the rotational speed (ω) and the derived outlet flow angle (β_2). Assumed given, as well, are the suction side velocity distribution and an approximate pressure side velocity distribution versus arc length. The number of blades and the pressure side velocity distribution will change during the computation, in order to obtain a closed profile, with the constraint to alter them as little as possible.

The flow is considered steady, inviscid, compressible subsonic and irrotational in the absolute frame of reference.

The physical plane is presented in figure 2a. The equations written on an axially symmetric system (m, θ) , are:

a) the continuity equation

$$\frac{\partial}{\partial m} (\rho R (\Delta n) W_m) + \frac{\partial}{R \partial \theta} (\rho R (\Delta n) W_u) = 0 \quad (1)$$

b) the absolute irrotational flow equation

$$\frac{1}{R} \frac{\partial (R W_u + \omega R^2)}{\partial m} - \frac{\partial W_m}{R \partial \theta} = 0 \quad (2)$$

In the previous version of the method (ref.[12]) a transformation is performed to the (Φ, Ψ) plane defined as

$$\vec{n} \times \nabla_s \Psi = \rho (\Delta n) \vec{W} \quad (3)$$

$$\nabla_s \Phi = (\vec{W} + \vec{\omega} \times \vec{R}) \quad (4)$$

where ∇_s is the surface gradient operator and \vec{n} the normal to the surface unit vector.

The difference $d\Phi$ along iso- Ψ lines is equal to

$$d\Phi = (\vec{W} + \vec{\omega} \times \vec{R}) d\vec{s} = W ds + \omega R^2 d\theta \quad (5)$$

This difference, however, is not always positive since there may exist certain high peripheral speed cases for which $d\Phi$ locally takes negative values and, thus, Φ is non-monotonic along streamlines. This fact prohibits the mapping of the physical coordinate plane to the potential/stream-function plane (the Jacobian of the transformation becomes zero) and thus no arithmetical solution is possible. To overcome this inconveniency, a new transformed plane (Φ, Ψ) is defined in the following way

$$\vec{n} \times \nabla_s \Psi = \rho (\Delta n) \vec{W} \quad (6)$$

$$\nabla_s \Phi_1 = \vec{W} + \vec{U} - (\vec{B}/R) \quad (7)$$

where \vec{B} is a vector parallel to the peripheral velocity \vec{U} and its modulus B is constant. The difference $d\Phi_1$ along a streamline is, then, equal to

$$d\Phi_1 = (\vec{W} + \vec{\omega} \times \vec{R} - \vec{B}/R) \cdot d\vec{s} = W ds + (\omega R^2 - B) d\theta \quad (8)$$

It is obvious that B can be selected in such a way that guarantees the positivity of the Jacobian of the transformation from the physical to the (Φ_1, Ψ) -plane.

On the (Φ_1, Ψ) -plane the equations of continuity and absolute irrotational flow can be written in the form

$$\begin{aligned} A_1(\ln W)_{\Phi_1 \Phi_1} + A_2(\ln W)_{\Phi_1}^2 + A_3(\ln W)_{\Phi_1} + A_4(\ln W)_{\Psi \Psi} + A_5(\ln W)_{\Psi}^2 + \\ A_6(\ln W)_{\Psi} + A_7(\ln W)_{\Phi_1 \Psi} + A_8(\ln W)_{\Phi_1} (\ln W)_{\Psi} + A_9 = 0 \end{aligned} \quad (9)$$

$$\frac{\partial \beta}{\partial \Psi} = F_1(W, \beta, R, (\Delta n)) \quad (10)$$

$$\frac{\partial \beta}{\partial \Phi_1} = F_2(W, \beta, R, (\Delta n)) \quad (11)$$

The expressions for the coefficients A_1 to A_9 are given in the reference [15]. In the above equations Φ_1 and Ψ are the independent variables, while the velocity modulus (W) and the flow angle (β) are the dependent ones. Equations (10) and (11) for the flow angle are equivalent so during the calculation one of them may be utilized.

THE BOUNDARY CONDITIONS ON THE (Φ_1, Ψ) -PLANE

The transformed plane- (Φ_1, Ψ) is presented in figure 2b. The flow quantities are known at station (1), inlet, and the flow angle at station (2), outlet. The integral mass flux conservation equation, the energy conservation equation along a meridional streamline and the isentropic flow relations are used to calculate flow quantities at station (2). The integral mass flux equation is written in the form

$$\rho_2 W_2 = \rho_1 W_2 \frac{R_1 \cos \beta_1 (\Delta n)_1}{R_2 \cos \beta_2 (\Delta n)_2} \quad (12)$$

and the energy conservation equation along with the isentropic flow relations results to the following expression

$$\frac{\rho_2}{\rho_1} = \left(1 + \frac{W_1^2 - U_1^2}{2c_p T_1} - \frac{W_2^2 - U_2^2}{2c_p T_1} \right)^{1/\gamma-1} \quad (13)$$

From these two equations the flow quantities (ρ_2, W_2) may be calculated for a known flow angle β_2 .

The integral momentum equation can be written in the form

$$\Gamma = \oint_{\text{blade}} \vec{V} d\vec{s} = \oint_{\text{blade}} W ds + \Gamma_1 = \frac{2\pi}{N} (R_1 V_{u1} - R_2 V_{u2}) \quad (14)$$

where

$$\Gamma_1 = \oint_{\text{blade}} \omega R^2 d\theta$$

This equation relates the flow conditions at the inlet and the outlet with the circulation Γ which depends on the velocity distributions along suction and pressure side, as well as, on the blade section geometry. Integral Γ_1 , depending on the blade section geometry, is not a priori known. This explains one of the difficulties of the inverse methodology applied to arbitrary rotating cascades. Note that Γ_1 is zero only when the radius R is constant. During the computational procedure the integral Γ_1 is given an initial reasonable value and corrected accordingly, each time a blade section shape is computed. In any case the value of Γ must be compatible with the imposed value of the outlet flow angle β_2 , so that, if the suction side velocity distribution (being most sensitive) must be maintained, the pressure side velocity distribution must be chosen to satisfy this value of Γ .

Considering, again, figure 2, periodic conditions are imposed along the ((AB),(EF)) and ((CD),(GH)) pairs of boundaries. $W(\Phi_1)$ is specified along the suction and pressure side solid boundaries and the corresponding value of Φ_1 is calculated from the following relation

$$d\Phi_1 = Wds + (\omega R^2 - B) d\theta \quad (15)$$

Consequently, differences in potential from a station ν to a station μ may be calculated as

$$\Delta\Phi_1 \Big|_{\nu}^{\mu} = \int_{\nu}^{\mu} Wds + \int_{\nu}^{\mu} (\omega R^2 - B) d\theta \quad (16)$$

Moreover, the way that the (Φ_1, Ψ) -plane was built assures that

$$\Delta\Phi_1 \Big|_A^B = \Delta\Phi_1 \Big|_E^F; \Delta\Phi_1 \Big|_B^C + \Delta\Phi_1 \Big|_G^F = \Gamma; \Delta\Phi_1 \Big|_C^D = \Delta\Phi_1 \Big|_G^H \quad (17)$$

During the computational procedure, the magnitudes of $\Delta\Phi_1 \Big|_A^B$ and $\Delta\Phi_1 \Big|_C^D$ are specified with the constraint to take them large enough in order to reach at AE and DH (see figure 2b) uniform conditions with sufficient accuracy. In this way, the position of the inlet and outlet of the calculation domain in the physical plane (positions of AE and DH in figure 2a) is not yet specified. However, using equation (4) along the peripheral direction one may get

$$d\Psi = \varrho(\Delta n) W \cos\beta R d\theta \quad (18)$$

so that the corresponding stream function differences are described by the following relation at the inlet and the outlet stations

$$\Delta\Psi \Big|_{\nu}^{\mu} = \int_{\nu}^{\mu} \varrho(\Delta n) W \cos\beta R d\theta \quad (19)$$

Along the inlet and outlet stations the flow is uniform with velocities and flow angles, W_1 , W_2 and β_1 , β_2 , respectively. Consequently, if $\Psi_E = \Psi_F = \Psi_G = \Psi_H = 0$ is the streamfunction value characterizing the lower boundary, then the one characterizing the upper boundary, according to equation (19), is

$$\Delta \Psi \left| \begin{array}{l} A \\ E \end{array} \right. = \rho_1 W_1 \cos \beta_1 \frac{2\pi R_1}{N} (\Delta n)_1 = \rho_2 W_2 \cos \beta_2 \frac{2\pi R_2}{N} (\Delta n)_2 = \Delta \Psi \left| \begin{array}{l} D \\ H \end{array} \right. \quad (20)$$

The upper boundary being a streamline, $\Psi_A = \Psi_B = \Psi_C = \Psi_D$.

THE NUMERICAL INTEGRATION OF THE EQUATIONS

Equations (9) and (10) or (11) are considered in the (Φ, Ψ) -plane, which in general is non-orthogonal. If one considers suction and pressure side extensions of equal length in the periodic zones (to facilitate the application of the periodicity conditions), then the computational domain on the (Φ, Ψ) -plane takes a trapezoidal form (see figure 2). A non uniform discretization of the (Φ, Ψ) boundary regions was found to be efficient, permitting the stretching of the grid lines in the near-leading and near-trailing edge regions of the blade section, where the velocity gradients are large. In view of the above, the resulting grid on the (Φ, Ψ) -plane, composed only of straight lines, is generally skewed and stretched. In order to increase the generality of the solver and the accuracy of the solution, avoiding at the same time complexities (such as patched grid techniques), an additional body-fitted coordinate transformation is performed, which maps the (Φ, Ψ) -plane to an orthogonal (ξ, η) -plane with square cells (see figure 2).

The resulting equation on W in the (ξ, η) -plane is discretized by use of second-order accurate finite-difference/ finite volume centered schemes. The discrete equation is, then, linearized, transferring all non-linear terms $((\ln W)^2)$, for example) to the right hand side (fixed point algorithm). The resulting system of algebraic equations, which has a 9-diagonal banded, non-symmetric characteristic matrix, is solved iteratively using the MSIP (refs [13],[14]) method (incomplete L-U approximate factorization procedure).

Once the velocity field is computed, the flow angle field is obtained integrating the ordinary differential equations (10) or (11), along the iso- Φ 1 or the iso- Ψ lines. A fourth order Runge-Kutta method is used during this step. In practice, equation (11) is first integrated along the cascade mean streamline and the computed β -mean streamline values are used as boundary conditions for the integration of equation (10) along the iso- Φ 1 lines. This procedure involves only a tangential derivation of the flow quantities along the blade and is, thus, more accurate. If a second order normal derivation along the blade is used, then quadratic extrapolation procedures would be required, decreasing the accuracy (mainly) in the sensitive leading edge region. The above procedure provides the complete $\beta(\Phi, \Psi)$ field and, consequently, the blade coordinates.

THE COMPUTATIONAL ALGORITHM

A computational algorithm was constructed, outlined by the following steps (without considering conditions for section closure, which will be examined later).

STEP 1 : The exit plane flow quantities are calculated through equations (12) and (13). A value for the integral Γ_1 is assumed and a velocity distribution for the pressure side compatible with the value of the circulation Γ issued from equation (14) is established. The value of constant B is defined so that Φ 1 is monotonic along streamlines. The values of the potential differences $\Delta \Phi 1 \Big|_A^B$ and $\Delta \Phi 1 \Big|_C^D$ are specified.

STEP 2 : A first approximation of the (Φ, Ψ) -plane contour is considered and the boundary conditions for the velocity (through equations (16) and (19)) and the angle (utilizing plausible angle distributions), are specified. The interior grid points of the region (BCGF) are established using a simple linear procedure. In the upstream (ABFE) and downstream (CDHG) regions, the points on the boundaries are chosen and the grid is constructed, so that periodic conditions can be checked without interpolation. The complete velocity and flow angle fields are initialized making use of the values at the boundaries, through a linear interpolation. An initial estimate of (Δn) and R for each node is made, as well.

STEP 3 : The coefficients $A_i (i=1,9)$ appearing in equation (9) are calculated.

STEP 4 : Equation (9) is solved for $W(\Phi, \Psi)$ using the numerical procedure and technique

described in the previous section. At this point, an iterative procedure is performed involving the previous step, that is, updating the values of the coefficients A_i . This updating is performed, utilizing the values of the velocity field of the previous iteration.

At the end of the computational procedure involved in this step, the values of W at the periodic boundaries will have been updated along with the complete velocity field.

STEP 5 : The flow angle field $\beta(\Phi, \Psi)$ is computed after numerical integration of equations (10) and/or (11) in the manner described in the previous section. During this procedure, new angle values are computed at the boundaries, as well.

STEP 6 : The blade section shape $\theta = \theta(m)$ is computed using the following geometrical relations, valid along a streamline

$$m = \int \cos\beta ds = m(s) \quad (21)$$

$$\theta = \int \frac{\sin\beta}{R} ds = \theta(s) \quad (22)$$

Utilizing these relations, the values of m and θ are computed along streamlines for the whole flow field, as well. An interpolation procedure is used in order to estimate the new set of values $R(m(s))$ and $\Delta n(m(s))$, which will be used, along with the updated values of the angles.

The exit conditions are calculated at station (2), using the same procedure as in STEP1. The integral Γ_1 is then computed and its new value is used to update Γ . The pressure side velocity distribution is in turn modified in order to satisfy the new value of the circulation. The B constant value is modified for the new geometry and velocity distribution. The boundaries and associated conditions can then be established for a new (Φ, Ψ) -plane. A new grid is thus generated on the (Φ, Ψ) -plane, moving along Ψ -lines and computing each time the value of Φ corresponding to the previously updated values of the velocity field.

STEP 7 : STEPS 3 to 6 are repeated until convergence is achieved.

As observed before, the blade section shape obtained from the above described computational procedure is not necessarily closed.

RESULTS AND DISCUSSION

To validate the method stationary and rotating cascade reconstruction test cases were selected. Exact cases were preferred where possible, while a direct solver was used to calculate the "target", velocity distribution when the later was not analytically known. Inevitably, slight inaccuracies in the results of the direct calculation method resulted in inaccuracies of the computed blade shape by the inverse method. A complete outline of the test cases utilized for the validation of the method are reported by Bonataki^[15]. Results for two analytical test cases and for a radial inflow turbine are presented below.

In figure 3 the Gostelow^[16] exact case (incompressible flow, compressor cascade) and in figure 4 the Hobson^[17] exact case (high Mach number, high turning angle, low pitch to chord ratio) are presented to demonstrate the accuracy of the method. A radial inflow turbine case^[18] (strong variation of $R(m)$, rotational, variation of $\Delta n(m)$) is presented in figure 5. In all three cases the presented results include the initial blade shape, the corresponding suction and pressure side velocity distribution and the blade shape provided by the inverse method. The typical number of grid points utilized for the above calculations was (78x15) and the computing time needed for the complete solution was 20 cpu seconds in an ALLIANT FX 80 computer.

As a next step the method was used for the design of new profiles. Starting from an arbitrary suction and pressure side velocity distribution, a procedure was developed which in few iterations provides a closed profile. This procedure is based on an extended investigation upon the parameters which influences the blade section shape^{[12],[15]}, an investigation which has pointed out that the ratio

of pressure to suction side arc length and the pitch to chord ratio could control blade section closure. It was also observed that the velocity distribution near the blade section edges influences a small part of the blade shape near these edges, while the blade thickness is directly related to the mean value of the velocity distributions along both the pressure and suction sides^[12]. Using the information provided by the above investigation new profiles were designed.

A rotating turbine cascade lying on a conical surface along with the "target" velocity distribution is presented in figure 6.

In figure 7 a turbine blade is presented, which was used as the starting point for the design of a thicker blade. This new blade was obtained by increasing the level of the suction and pressure side velocity distributions while retaining the same inlet and outlet flow conditions. This particular design is quite revealing, since the "target" velocity was obtained by modifying the original one in such a way, so that the maximum velocity along the blade surfaces was not increased.

The blade section shape of a radial inflow turbine with speed of rotation is presented in figure 8a along with the corresponding $R(m)$ and $\Delta n(m)$ distributions (figures 8c,8d) and "target" velocity distribution (figure 8b). This is a typical case where the classical (Φ, Ψ) plane definition fails and this is demonstrated in figures 8e,8f where the (Φ, Ψ) -plane is plotted for two different values of the B parameter, $B=0$ (the classical Φ definition) and $B=1.1$ (the modified definition). It is evident that the modified definition suits better to the specific case.

CONCLUSIONS

A new inverse inviscid method for designing stationary or rotating, plane or axisymmetric cascades was presented in this paper.

Compared with previous efforts, the new method may handle cascades rotating with high speed and provide closed blade shapes in few external iterations.

The formulation and the numerics of the corresponding inverse method were discussed, in order to distinguish it from similar methods and reveal its relative merits.

Finally, some calculation results were presented, to certify the accuracy and the capabilities of the present effort.

REFERENCES

1. International Conference on Inverse Design Concepts in Engineering Sciences (ICIDES-I), Aero. Eng. Dept., University of Texas, Austin, TX, Oct. 17-18, 1984.
2. International Conference on Inverse Design Concepts and Optimization in Engineering Sciences (ICIDES-II), Aero. Eng. Dept., Penn State Univ., University Park, Oct.26-28, 1987.
3. AGARD Specialist's Meeting on Computational Methods for Aerodynamic Design (Inverse) and Optimization, Loen, Norway, May 24-25, 1989.
4. AGARD Lecture Series 167, Blading Design for Axial Turbomachines, Lyon, France, 19-20 June, 1989.
5. AGARD VKI Special Course on Inverse Methods in Airfoil Design, Rhode-Saint-Genese, Belgium, 14-18 May, 1990.
6. STANITZ J.D., "Design of Two-Dimensional Channels with Prescribed Velocity Distributions along the Channel Walls", NACA report 1115, 1953.
7. SCHMIDT E., "Computation of Supercritical Compressor and Turbine Cascades With a Design Method for Transonic Flows", Trans. of ASME, Jr. of Engg. for Power, Vol.102, pp.68-74, Jan.1980.
8. SCHMIDT E., BERGER P., "Inverse Design of Supercritical Nozzles and Cascades", Int. J. Num. Meth. Eng., Vol. 22, Feb. 1986, pp. 417-432.
9. SCHMIDT E., "Inverse Methods for Blade Design, Controlled Diffusion Blading for Supercritical Compressor Flow", VKI-LS 1988-03 Transonic Compressors.
10. SCHMIDT E., KLIMETZEK F., "Inverse Computation of Transonic Internal Flows With Application for Multi-Point-Design of Supercritical Compressor Blades", Presented at the Specialists Meeting on Computational Methods for Aerodynamic Design (Inverse) and

- Optimization, Loen, Norway, May 1989.
11. ZANNETTI L., "A Natural Formulation for the Solution of Two-Dimensional or Axisymmetric Inverse Problems", *Int. J. Num. Meth. Eng.*, Vol.22, Feb.1986, pp.451-463.
 12. BONATAKI E., CHAVIAROPOULOS P., PAPAILIOU K.D., "An Inverse Inviscid Method for the Design of Quasi-Three Dimensional Turbomachinery Cascades", presented at the International Symposium on Numerical Simulations in Turbomachinery Joint ASME-JSME Fluids Engineering Meeting, Oregon, June 23-26, 1991.
 13. ZEDAN M. SCHNEIDER G.E., "A Three-Dimensional Modified Strongly Implicit Procedure for Heat Conduction", *AIAA Journal*, Vol. 21, 1983.
 14. CHAVIAROPOULOS P., GIANNAKOGLOU K., PAPAILIOU K.D., "Numerical Computation of Three-Dimensional Rotational Inviscid Subsonic Flows, Using the Decomposition of the Flow Field into a Potential and a Rotational Part", ASME paper 86-GT-169.
 15. BONATAKI E., "Inviscid Subsonic Inverse Method for the Design of Blade Sections along Arbitrary Axisymmetric Stream Surfaces with Varying Stream Tube Width", Ph.D.Thesis, in preparation, NTUA, Greece.
 16. GOSTELOW J.P., "Potential Flow Through Cascades -A Comparison Between Exact and Approximate Solutions", A.R.C., CP No 807, 1963.
 17. JONES D.J., "Test Cases for Inviscid Flow Field Methods, Reference Test Cases and Contributors", AGARD AR-211.
 18. KATSANIS T., "Fortran Program for Calculating Transonic Velocities on a Blade-to-Blade Stream Surface of a Turbomachine", NASA TN D-5427, 1969.
 19. BOURAS B., KARAGIANNIS F., CHAVIAROPOULOS P., PAPAILIOU K.D., "Arbitrary Blade Section Design Based on Viscous Considerations. Blade Optimization", presented at the International Symposium on Numerical Simulations in Turbomachinery Joint ASME-JSME Fluids Engineering Meeting, Portland, Oregon, June 23-26, 1991.

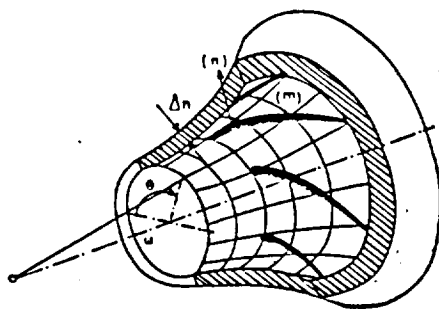
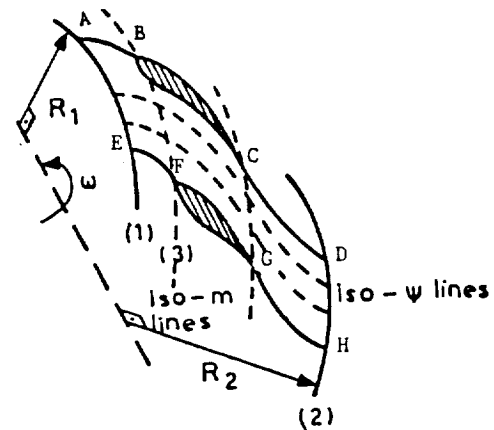
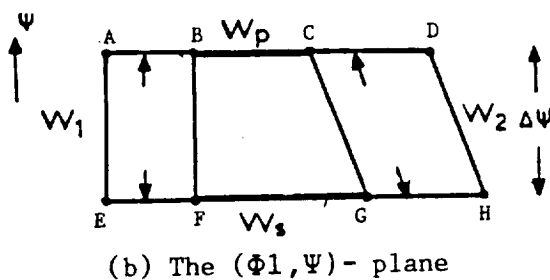


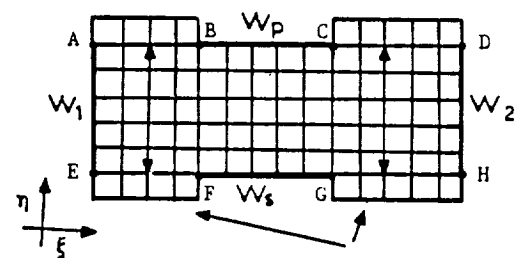
Fig.1 A schematic representation of a peripheral cascade



(a) The physical plane

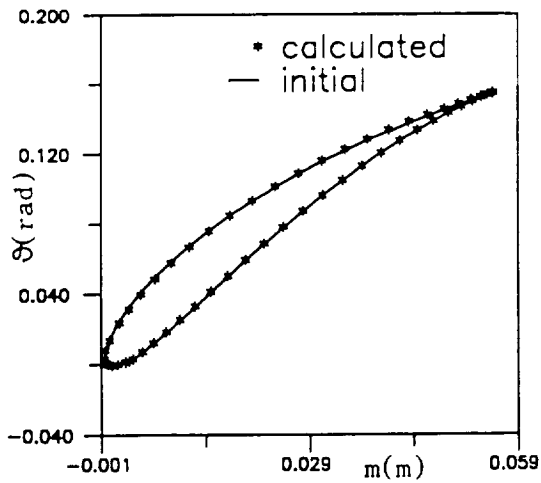


(b) The (Φ_1, Ψ) - plane

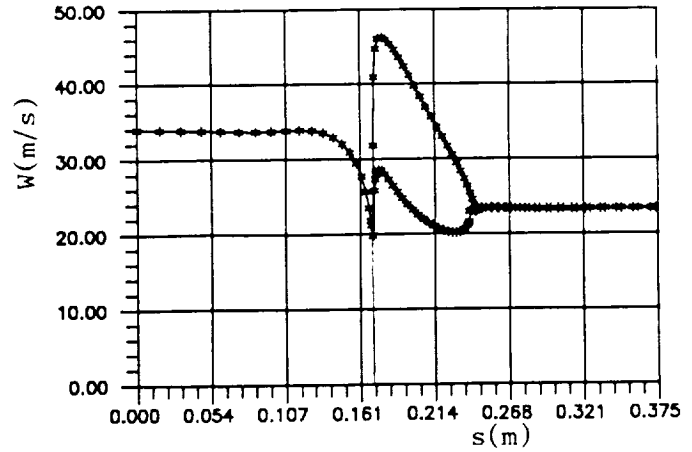


(c) The computational plane

Fig.2 The schematic representation of a blade passage of a peripheral cascade

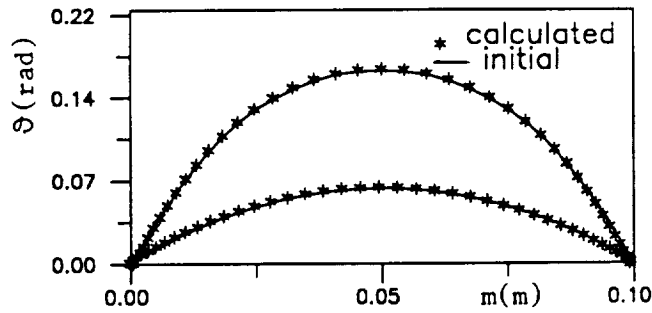


(a) The initial and recalculated blade shape

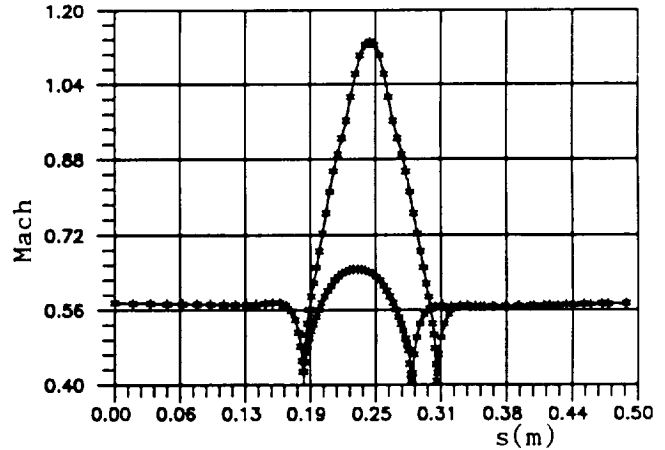


(b) The velocity distributions

Fig.3 The Gostelow cascade

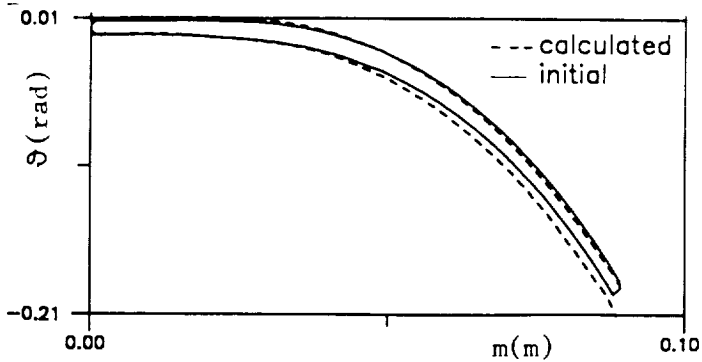


(a) The initial and recalculated blade shape

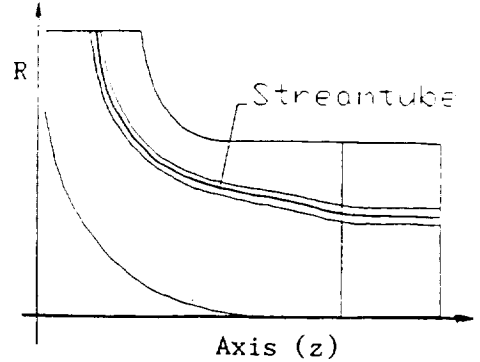


(b) The Mach number distributions

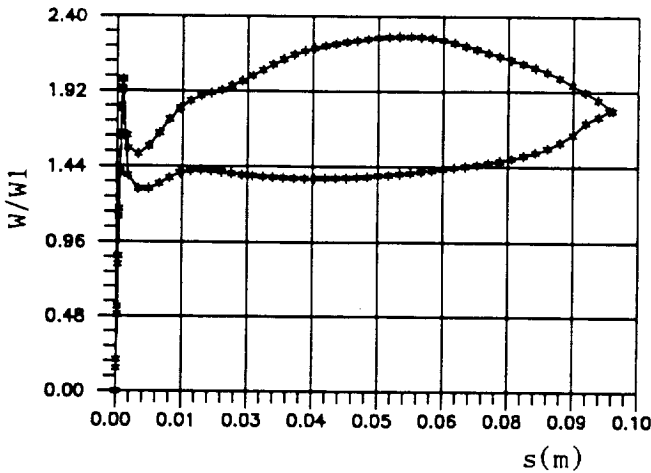
Fig.4 The Hobson cascade



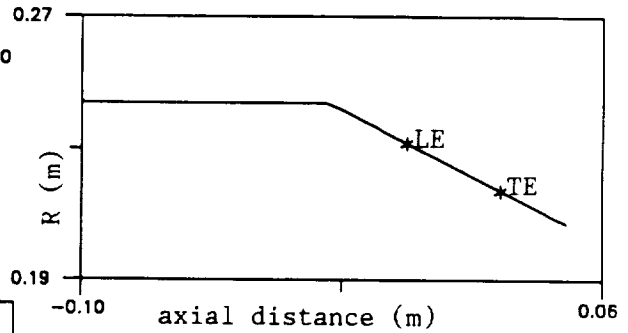
(a) The initial and recalculated blade shape



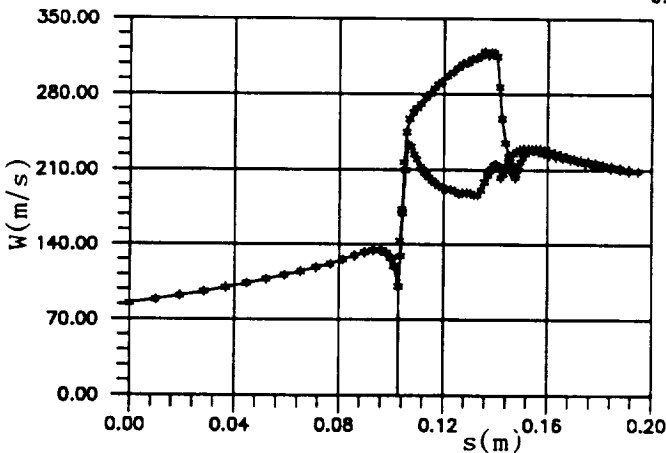
(c) The meridional plane and the streamtube variation



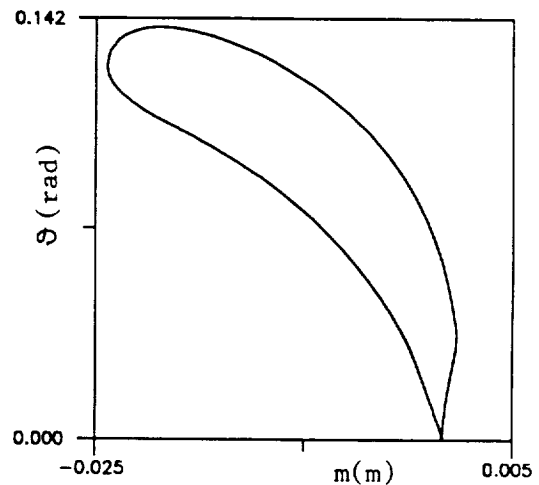
(b) The velocity distributions



(a) The generatrix of the axisymmetric streamsurface



(b) The velocity distributions



(c) The calculated profile

Fig.6 Design of a new rotating cascade

Fig.5 A rotating turbine case

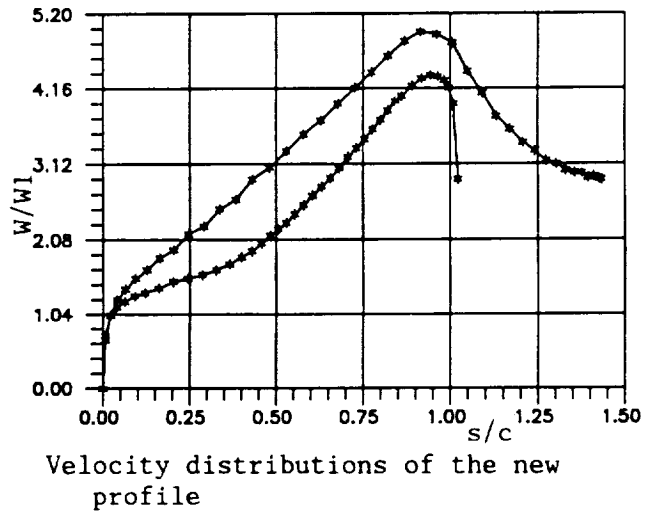
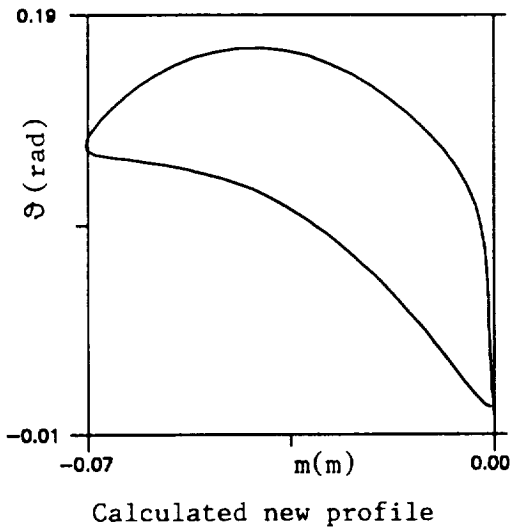
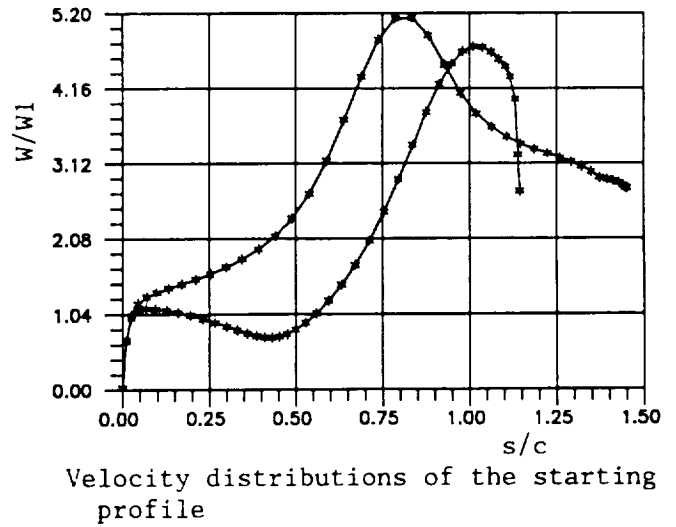
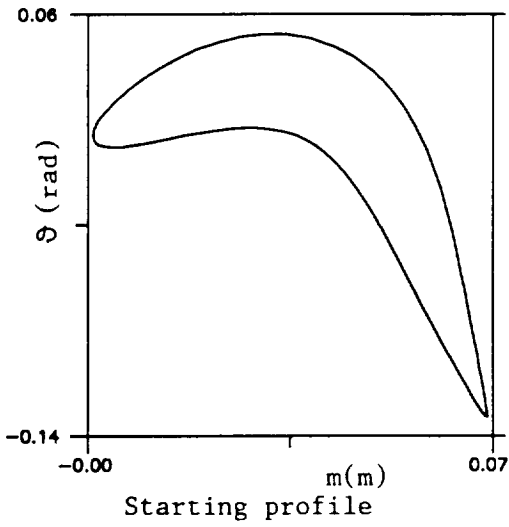
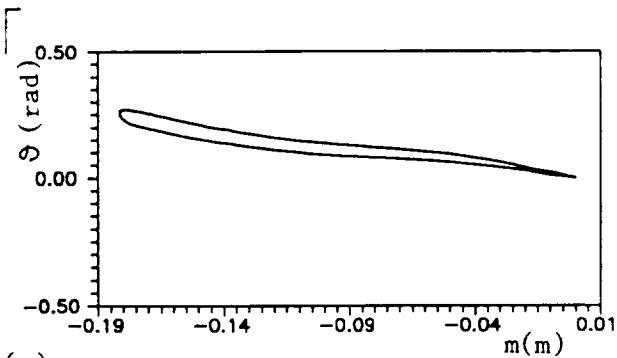
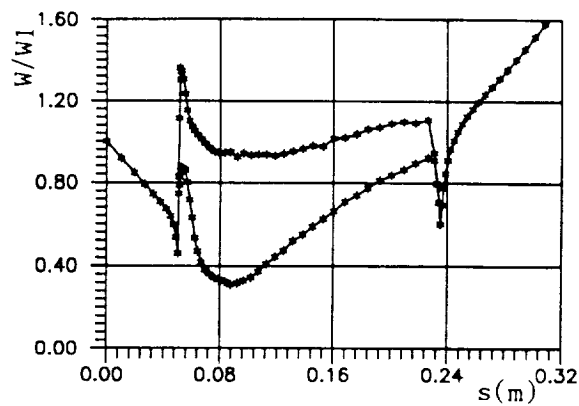


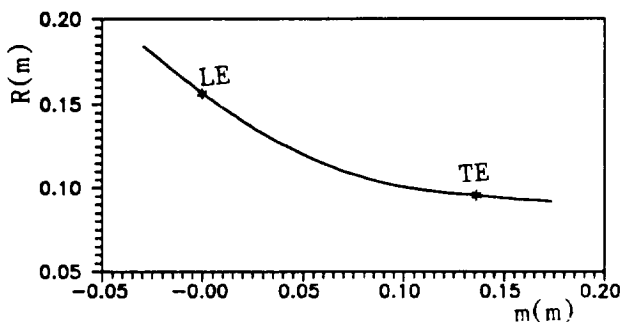
Fig.7 Design of a thicker profile



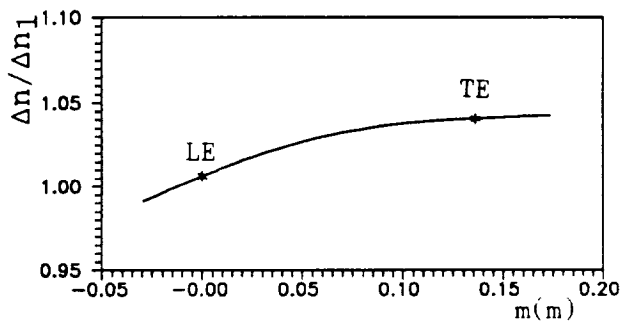
(a) The calculated profile



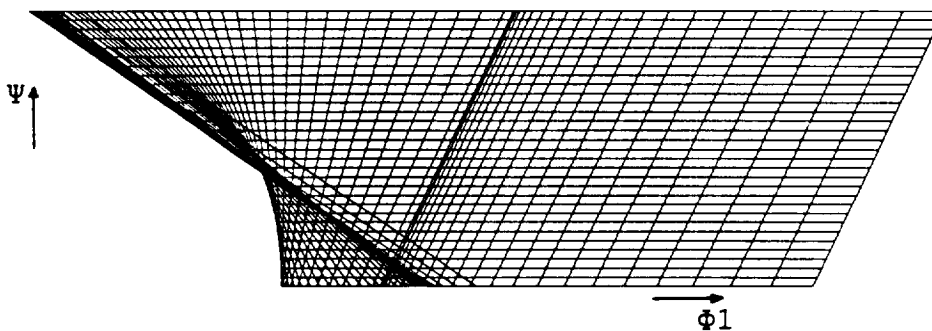
(b) The velocity distributions



(c) The radius variation with the meridional distance



(d) The streamtube thickness variation with the meridional distance



(e) The grid on the (Φ_1, Ψ) -plane for $B=0$ ($\Phi_1 = \Phi$)



(f) The modified grid on the (Φ_1, Ψ) -plane for $B=1.1$

Fig.8 Design of a radial inflow turbine